Tapping Mode Atomic Force Microscopy on Polymers: Where Is the True Sample Surface?

A. Knoll,[†] R. Magerle,[†] and G. Krausch*,[†,‡]

Physikalische Chemie II, Universität Bayreuth, 95440 Bayreuth, Germany, and Bayreuther Zentrum für Kolloide und Grenzflächen (BZKG), Universität Bayreuth, 95440 Bayreuth, Germany

Received July 25, 2000; Revised Manuscript Received February 7, 2001

ABSTRACT: We investigate in detail the processes involved when soft polymeric materials are imaged with TappingMode atomic force microscopy (TM-AFM). Measuring lateral arrays of amplitude/phase vs distance (APD) curves, we are able to determine quantitatively the amount of tip indentation and reconstruct the shape of the "real" surface of the sample. Moreover, contrast inversion in height and TappingMode phase images is explained on the basis of attractive and repulsive contributions to the tip−sample interaction. The experiments are performed on surfaces of poly(styrene-*block*-butadiene-*block*-styrene) (SBS) triblock copolymers acting as a model system.

Introduction

TappingMode atomic force microscopy (TM-AFM)[1−3] has been established in recent years as a standard tool to investigate surfaces of soft materials. Its excellent lateral resolution together with its potential to distinguish different materials without further staining has made TM-AFM an attractive alternative to established techniques such as transmission electron microscopy. Despite its widespread use, however, the complex dependence of TM-AFM images on the imaging parameters[4] gives rise to the notion that the results may be subject to various uncontrolled artifacts and raises the question whether and how reproducible imaging conditions can be established. Typical problems occurring when TM-AFM is applied to polymeric samples concern the quantitative reproducibility of height and phase images, the distinction between real surface topography and indentation,[5] and even the frequently occurring contrast inversion of height and phase images.[4,6−8] In the present work, we apply TM-AFM to a typical heterogeneous block copolymer surface. Recent theoretical[9−11] and experimental work[12−15] has shown that the near-surface microdomain structure of block copolymers can differ significantly from the bulk situation. As a model material, we use a commercial poly(styrene-*block*-butadiene-*block*-styrene) (SBS) triblock copolymer. We present a simple means to distinguish between tip indentation and real surface topography and describe in detail the dependence of the resulting height and phase images on the imaging parameters.

In TappingMode (ref 2), the AFM cantilever is excited to a mechanical oscillation near its resonance frequency. Typical amplitudes A_0 at the tip side of the freely oscillating cantilever are some 10 nm. With typical spring constants of the cantilever of about 50 N/m, adhesive forces can be overcome, and an almost free oscillation of the cantilever is realized with the tip touching the surface only during a small fraction of each oscillation period. In consequence, lateral forces are minimized, and damage of the specimen is largely avoided with hardly any loss in lateral resolution. The interaction of the tip with the surface leads to a change of the amplitude A of the oscillation. The latter is detected and kept at a constant value (referred to as *set point* A/A_0) through a feedback mechanism continuously adjusting the distance between the cantilever and the surface under study. Changes in the position of the sample (or the cantilever) needed to keep a constant amplitude of oscillation are monitored and displayed as what is typically called a *topography* or *height image* of the surface.

In addition, the phase difference between the free end of the cantilever and the driving piezo element can be measured as well. The resulting *phase images* are discussed quite extensively in the recent literature.[16−22] Following a suggestion by Cleveland et al.,[23] the phase shift can be related to the power dissipated by the sample during the mechanical contact with the tip. It is generally accepted that the phase signal to some extent reflects the viscoelastic properties of the sample.[16] It is therefore often used to qualitatively distinguish different materials on the surfaces of heterogeneous samples. Quantitative information about materials constants, however, can hardly be extracted from phase images at present.

One reason for this deficiency is the fact that the time of contact between tip and sample is increasing with decreasing *set point*.[16] Therefore, the choice of the *set point* affects both the relative phase and the relative height signal on a heterogeneous sample. Under certain conditions, an inversion of the phase and height contrast can occur as the *set point* is changed. One way to quantitatively examine this dependence is to determine the amplitude and phase signals as a function of the distance between cantilever and sample (referred to as "APD curves"). Chen et al.[24,25] measured APD curves on gelatin, polystyrene, and mica samples and compared the respective results. The authors discussed height artifacts and phase contrast reversal on the basis of single APD curves measured on the different materials. Bar et al.[26] examined in this way polybutadiene/polystyrene-*co*-polybutadiene rubber blends.

In the present paper, we extend this work by determining APD curves as a function of the lateral position on a block copolymer surface exhibiting lateral heterogeneities on the 10 nm scale. Thereby we can compare

[†] Physikalische Chemie II.
[‡] Bayreuther Zentrum für Kolloide und Grenzflächen (BZKG).

10.1021/ma001311x CCC: $20.00
Published on Web 05/05/2001

the information contained in the APD curves directly to conventional TM-AFM images taken at the same spot of the sample. Furthermore, information about the surface can be extracted from the APD curves without the influence of the tapping conditions, and possible artifacts on the height image can be discussed. The indentation of the tip into the sample is determined quantitatively from the APD curves, and a model of the volume composition near the block copolymer surface can be estimated.

Experimental Section

All measurements were performed under ambient conditions using a commercial scanning probe microscope (Digital Instruments NanoScope Dimension 3100). A *single* silicon cantilever (NANO*SENSORS*, typical spring constant: 40 N/m) was used for all measurements in order to avoid possible artifacts due to differences in tip shape or spring constant. The parameters of the cantilever oscillation were determined by fitting a simple harmonic oscillator model to the amplitude vs frequency curves measured at a distance of about 100 nm above the sample surface. This distance is controlled by disabling the feedback loop of the instrument being in light tapping and subsequently retracting the tip and performing the frequency sweep. The resonance frequency and the quality factor of the cantilever were determined to 336.0 kHz and 365, respectively. It is worth mentioning that these values differ significantly at larger distances from the surface (336.4 kHz and 460, respectively, at 1 mm).

Quantitative measurements with TM-AFM rely upon a good calibration of the cantilever amplitude to the photodiode signal. In this work we used a procedure suggested by Nony et al.:[20] A series of APD curves are measured on the sample for different drive amplitudes of the piezo element exciting the cantilever oscillation, and the root-mean-square (rms) value P_{rms} of the photodiode signal is monitored. For each curve one determines the absolute position z_0 of the piezo element adjusting the cantilever sample distance when the tip first touches the sample (see below). The calibration factor is determined from the slope of the z_0 vs P_{rms} curve. Another way of calibrating the amplitude is measuring the decrease of the amplitude while approaching a hard surface (e.g., silicon). Both procedures resulted in a calibration factor of 23.7 ± 0.3 nm/V.

In the instrument used in this work the phase signal is generated by multiplying the normalized cantilever excitation signal with the normalized photodiode signal. This signal is closely related to the physical phase of the oscillation but has a value of zero at the resonance frequency of the cantilever. In this work we used this signal without any transformations as a measure of the physical phase.

Poly(styrene-*block*-butadiene-*block*-styrene) (SBS) was obtained from Polymer Source Inc. The PS, PB, and PS blocks had weight-averaged molecular weights of 14K, 73K, and 15K, respectively, and a polydispersity of 1.02. In bulk the PS blocks self-organize into cylinders of about 25 nm diameter embedded within a PB matrix. Viewed along their long axes the cylinders form a hexagonal lattice with a mean distance of 45 nm between two next-nearest cylinders. An SBS film was prepared on a polished silicon wafer by spin-casting (2000 rpm) from a 2 wt % toluene solution, which results in a film thickness of about 100 nm. For equilibration and long-range ordering of the SBS microdomain structure the sample was exposed to chloroform vapor.[27,28] The vapor pressure was reduced from about 80% of saturation to zero over 1 day. This procedure results reproducibly in films of about the same thickness with cylinders oriented parallel to the plane of the film.

The Nanoscope III software supplied with the instrument provides a means to measure an array of amplitude/phase-distance (APD) curves. In the present work an array of 30 × 30 curves with a lateral separation of 4 nm was measured within a total time of some 8 min. The resulting 900 curves were analyzed with home-built software (see below).

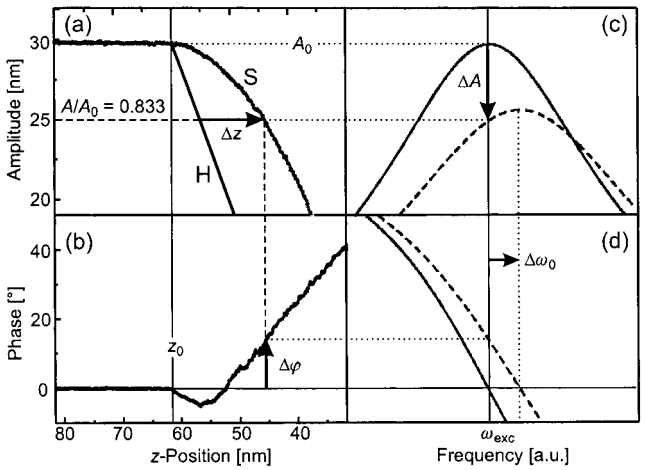

Figure 1. Typical amplitude vs distance (a) and phase vs distance curve (b) measured on the SBS sample. The straight line H represents an infinitely hard surface. Dashed lines indicate how indentation Δz and phase shift $\Delta\varphi$ are determined for a given set point A/A_0. (c, d) Cantilever amplitude and phase as a function of excitation frequency measured for the free oscillation (solid line) and for a cantilever in repulsive contact with the sample corresponding to a set point $A/A_0 = 0.833$ (dashed line) calculated based on a harmonic oscillator model. In contact the resonance frequency is shifted by $\Delta\omega_0$, and the quality factor is reduced, resulting in an amplitude reduction ΔA and a phase shift $\Delta\varphi$ at the excitation frequency ω_{exc}.

Results and Discussion

Figure 1 shows the typical behavior of amplitude (a) and phase (b) of the cantilever oscillation, when the tip approaches the surface. In this study only approach curves are used. At larger distances between tip and sample ($z > z_0$ in Figure 1a,b), both amplitude and phase are constant, indicating that in this regime the forces acting on the cantilever are negligible or distance independent. At a certain point z_0 the phase signal exhibits a kink and turns to negative values. At about the same *z*-position the amplitude starts to decrease. On further approach the amplitude signal continues to decrease while the phase signal eventually starts to increase.

This behavior can be explained with a model accounting for the additional forces introduced by the tip−sample interaction.[21,22,29] Within this model it is assumed that these forces are weak and can be considered as a perturbation of the mechanically oscillating system. In this case additional attractive (repulsive) conservative forces result in an decrease (increase) of the force constant of the oscillator, which in turn lead to a negative (positive) shift $\Delta\omega_0$ of the resonance frequency of the tip−sample system. In addition, energy dissipation into the sample will result in an increased damping of the system, i.e., in a decrease of the quality factor. In Figure 1c,d the amplitude and phase behavior for the free cantilever (solid lines) is shown together with a model resonance curve (dotted lines) of a harmonic oscillator assuming a positive shift of the resonance frequency and an increased damping. The latter serves as a model for a cantilever in (repulsive) contact with the sample. For a given *set point* the change of the resonance curve affects both amplitude and phase values at the excitation frequency ω_{exc}. In our experiment, the cantilever was excited (ω_{exc}) at its resonance frequency ω_0. The figure demonstrates how a net repulsive, dissipative force leads to a decrease of the

amplitude ΔA and an increase of the phase value $\Delta\varphi$ at the excitation frequency ω_{exc}. The dotted curves correspond to a set point $A/A_0 = 0.833$, i.e., a cantilever amplitude $A = 25$ nm. It becomes clear from the figure that the sign of the phase shift $\Delta\varphi$ indicates whether attractive or repulsive forces govern the tip sample interaction.

Returning to the experimental APD curves displayed in Figure 1a, we can identify the initial decrease of the phase values as the result of attractive forces between tip and sample. Attractive forces are expected to result from long-range van der Waals interactions[18−20] and adhesive contributions including capillary forces.[30] The increase of the phase signal at smaller tip−sample distances can be attributed to increasing repulsive forces due to the indentation of the tip into the sample.

One major problem in TM-AFM on soft materials is the distinction between the real surface topography and an apparent one due to lateral variations of the indentation depth of the tip.[5] One therefore faces the problem to define at which *z*-position the tip touches the surface. In the present work we chose the initial kink in the phase signal as this point z_0 in all APD curves.[31,32] This choice seems reasonable assuming that long-range attractive forces are independent of the lateral position of the tip. This assumption seems justified on our particular sample, since van der Waals forces will be similar for the two components of the block copolymer under study. Therefore, we may at worst introduce a systematic error at this point which does not effect the general conclusions drawn in the following discussion.

When the tip touches the surface, i.e., around $z = z_0$, the amplitude signal shows a much weaker effect than the phase signal. The rather soft sample allows the tip to indent the surface, which results in a smoothly varying amplitude signal. If the sample would be infinitely hard, the amplitude of the cantilever oscillation would decrease linearly as the cantilever base is getting closer to the surface. This behavior is indicated by the straight line H in Figure 1a. At any given *set point* A/A_0, the indentation Δz of the tip is given[5] by the difference in *z* when the amplitude reaches the *set point* value on the soft sample (S) and the ideally hard surface (H) (horizontal arrow in Figure 1a). We note that this measurement of the indentation relies on two assumptions. Since only the rms value of the oscillation is measured, one has to assume that the oscillation of the cantilever remains harmonic even when it is in contact with the sample surface. This assumption has been found to be valid on soft samples.[23,33] Second, the average deflection of the cantilever has to be zero. This can be measured by monitoring the dc offset of the photodiode signal, and it was found that the signal is negligible in the measured *z* range.

On the basis of the above considerations, we are now able to determine the shape $z_0(x,y)$ of the physical surface of our block copolymer sample and to quantitatively determine lateral maps of tip indentation $\Delta z(x,y)$ for any given *set point*. A 30 × 30 array of APD curves was measured on an SBS sample. This procedure enables us to directly compare surface morphology and indentation maps to the common height images obtained in a standard TM-AFM experiment performed at the same spot of the sample. In addition, images of the phase shifts can be reconstructed from the APD curves and compared to TM-AFM phase images.

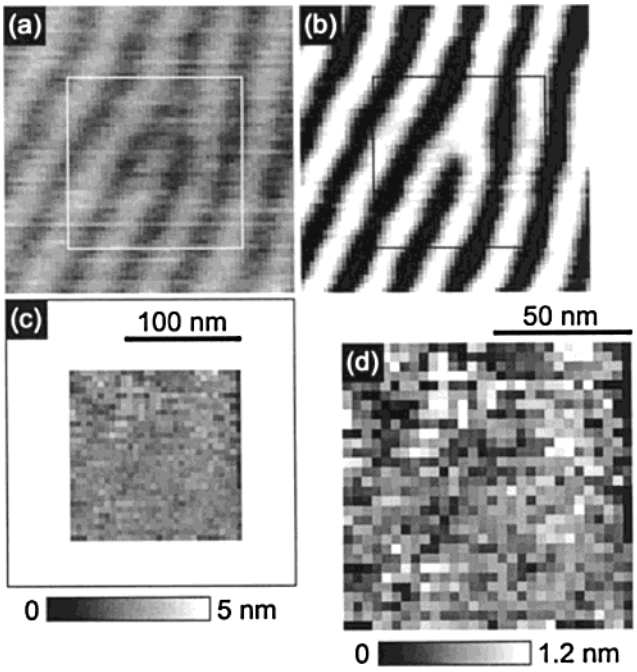

Figure 2. Height images measured with conventional TM-AFM ($A_0 = 30$ nm) at set points $A/A_0 = 0.99$ (a) and 0.70 (b). (c, d) "Real surface topography" z_0 of the area indicated by the box in (a) reconstructed from the APD curves. In (a), (b), and (c) the same height scale has been chosen (0−5 nm), while in (d) the height scale is blown up to 0−1.2 nm.

We start with the reconstruction of the surface topography $z_0(x,y)$ from the absolute *z*-positions of the *z*-piezo element when the cantilever comes into contact with the sample. Figure 2 shows a comparison of conventional TM-AFM height images taken at *set points* $A/A_0 = 0.99$ (a) and 0.70 (b). In addition, we show the surface topography $z_0(x,y)$ of the same spot of the sample reconstructed from APD curves in the same height scale (0−5 nm) (Figure 2c). Figure 2d shows the same data with the height scale blown up to 0−1.2 nm. The TM-AFM height images show a stripelike pattern at both *set points*, indicative of a regular hill and valley morphology on the surface. Dependent on the *set point* value, however, the height contrast is inverted; i.e., hills observed at $A/A_0 = 0.99$ turn into valleys at $A/A_0 = 0.70$ and vice versa. The reconstruction of the surface topography from the APD curves (Figure 2c) indicates that the polymer surface is essentially flat with a surface roughness less than 1 nm. As can be seen from Figure 2d, the surface roughness (fwhm of z_0 histogram = 0.6 nm) is of the order of the uncertainty of the z_0 determination.

Using the procedure described above for calculating indentation and phase values for a given *set point*, one can calculate indentation and phase images. To compare these pictures to regular TM-AFM images, a set of TM-AFM images was taken with the same tip at the same spot of the sample using *set points* between $A/A_0 = 0.99$ and 0.50. At *set points* smaller than 0.50 the imaging conditions became unstable, resulting in distorted TM-AFM images. A comparison between the conventional TM-AFM images and the images reconstructed from the APD array is shown in Figure 3. In the left part the indentation maps (a) are compared to the TM-AFM height images (b) at the respective *set point* values. Note that the indentation scale is an absolute scale while the height scale in TM-AFM is only a relative measurement.

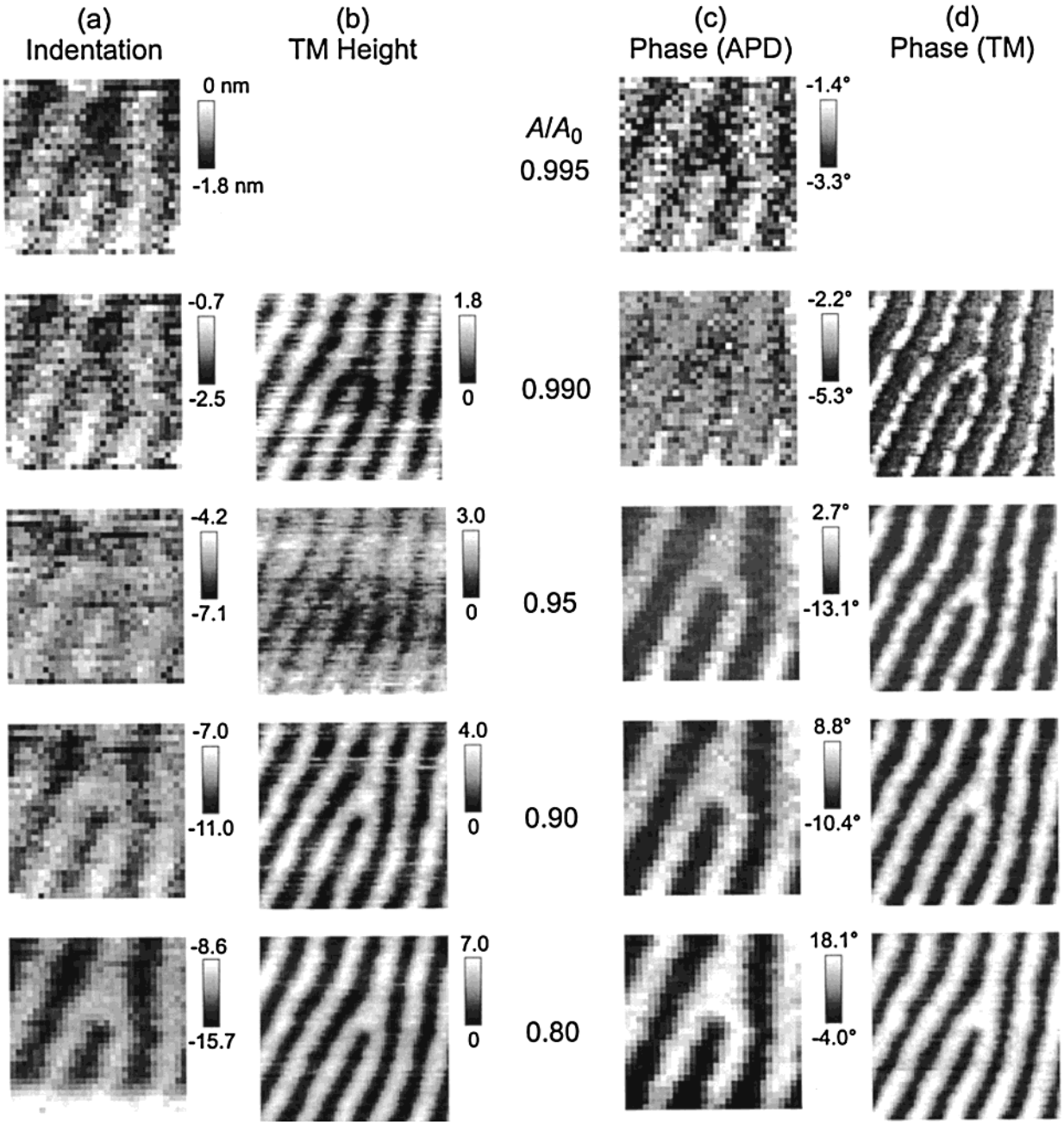

Figure 3. Comparison of indentation (a) and phase signal (c) determined from APD curves (imaged area = 120 × 120 nm^2) with the respective TM-AFM height (b) and phase (d) images (250 × 250 nm^2) taken at different *set points* A/A_0 ranging from 0.995 to 0.80 (A_0 = 30 nm). Note that only the central part of the area imaged by conventional TM-AFM (b, d) is reconstructed from the APD curves (a, c).

Therefore, only the difference of maximum and minimum values in the scales can be chosen equal. In the right-hand part of Figure 3, the phase images obtained from the APD curves (c) are compared to the conventional TM-AFM phase images (d). The scales of the images are the same for the corresponding *set points*; therefore, only a single scale bar is shown. It can be seen that the indentation maps and the phase images based on the APD curves correspond very well to the respective TM-AFM height and phase images. The striking result of this comparison is the observation that, for the particular sample under study, the conventional TM-AFM "height images" merely reflect lateral differences in tip indentation depth on a virtually flat sample. They are not related to the real surface topography. In general, TM-AFM height images will be determined by an interplay between real surface topography and indentation. The procedure described above is able to distinguish and to determine quantitatively the two contributions.

The absolute amount of indentation is surprisingly high, taking into account the free amplitude A_0 = 30 nm. To further elucidate this point, Figure 4 shows another plot of the indentation depth and the phase shift as a function of the *set point* for five APD curves taken at different lateral positions showing very high and very low absolute indentations. Given the different rheological properties of PS and PB at room temperature, we identify the regions of high indentation with PB-rich microdomains located near the surface, while the smaller indentation is expected in the vicinity of PS-rich microdomains. Together with the APD data, we show amplitude and phase values taken from TM-AFM images in the following way: The open symbols were obtained as

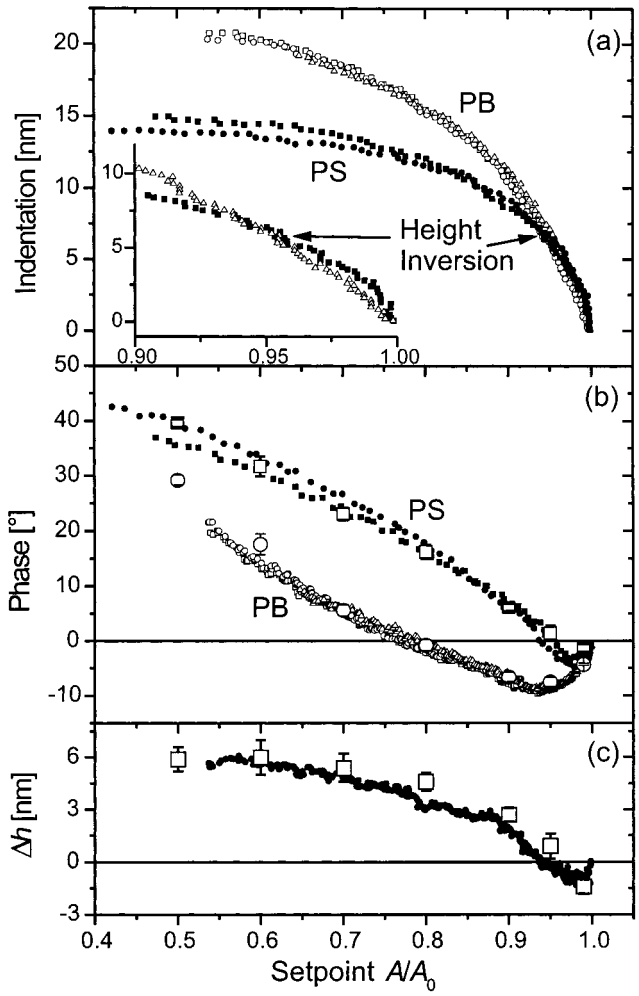

Figure 4. Indentation (a) and phase signal (b) vs set point A/A_0 taken in the center of PS- and PB-rich areas (A_0 = 30 nm). The crossing of the indentation signals at A/A_0 = 0.95 indicates the height inversion in a TM-AFM experiment. In (b) the large open symbols and error bars represent average values extracted from 10 scan lines taken from the TM-AFM height and phase images. (c) Height difference Δh (open symbols) between PS- and PB-rich areas in TM-AFM height images and differences in indentation (closed symbols) between PS and PB-rich areas determined from APD data shown in (a).

average maxima and minima of 10 scan lines taken perpendicular to the direction of the stripes. The error bars represent the standard deviations of these values. Since only height differences Δh are measured in TM-AFM (see Figure 4c) the difference in indention (determined from the average of the respective curves shown in Figure 4a) is shown for comparison. Figure 4b,c shows that the data obtained with both methods agree quantitatively in the measured regime. On the softer parts of the sample the indentation reaches values as high as 20 nm. This corresponds to 66% of the free cantilever amplitude A at a *set point* A/A_0 of about 0.5, which in turn relates to a cantilever amplitude A of about 15 nm. This finding implies that the tip is in contact with the sample more than half of its oscillation period.

As expected, the indentation increases with decreasing *set point*. On the harder parts of the surface the indentation levels off at about 15 nm. Interestingly, at high *set points* the increase of indentation with decreasing *set point* is faster on the harder parts as compared to the softer parts of the sample. Consequently, the indentation curves cross at a *set point* A/A_0 of about 0.95. In the TM height images this behavior appears as an inversion of the height contrast between the two materials (see Figure 2a,b). As a possible physical explanation of this effect, one needs to consider the fact that PB is liquid at room temperature and therefore is expected to strongly adhere to the tip. This adhesion will effectively damp the cantilever oscillation leading to the observed steep decrease in amplitude as the tip approaches the sample. At lower *set points* repulsive contributions will eventually dominate, and the harder material (PS) will show larger decrease in amplitude (i.e., smaller indentation).

The phase signal at lower *set points* rises much faster on the harder (PS-rich) phase. In TM-AFM this typically results in a phase contrast with the polystyrene part appearing brighter. In this regime the repulsive forces between the tip and the sample dominate. It has been stated that the difference in the phase signal cannot be explained by simply assuming different material constants of the constituent materials.[16] This, however, is true only if damping is neglected. If the damping constant of both materials happens to be similar, the harder material will shift the phase to higher values because it introduces the higher additive force constant to the system. In this particular experiment no phase inversion could be detected in the TM-AFM images. The APD curves display a phase inversion at very high *set points*, where stable TM-AFM imaging was hardly possible. This phase inversion in the purely attractive regime could again result from a higher adhesion hysteresis of the butadiene phase.

At this point we like to report on the reproducibility of our results. Comparable experiments with different tips and different free amplitudes between 20 and 40 nm have been done. The behavior of indentation, height, and phase vs *set point* A/A_0 (as shown in Figures 2, 3, and 4) is very reproducible as long as "fresh and clean" tips from the same tip wafer are used on identically prepared SBS samples. In these cases and within the *set point* range 0.5−0.95 indentation increases systematically with increasing free amplitude A_0 and decreasing *set point* A/A_0. For PS, *set point* A/A_0 = 0.75, and free amplitude A_0 between 20 and 40 nm, for example, indentation varies (almost linear) between 7 and 18 nm. Variations from tip to tip are in the range of ±10%. For *set points* close to 1.0 reproducibility is limited by the amplitude noise. Similar holds for the phase vs *set point* curves. For PS for instance, the minimum value of the phase varies by ±10% and is always reached within the *set point* range of 0.99 and 0.96. AFM tips get "dirty" or dull after some time of scanning. This happens more frequently when high scan speeds are used or when hard surfaces such as Si are scanned with set points < 0.5. In these cases we observe that indentation is considerably reduced. Also, the contrast in conventional TM-AFM phase images is drastically reduced (if not lost), and phase vs distance curves change considerable while keeping qualitatively their shape. Apparently, indentation and phase vs *set point* curves depend critically on tip shape. However, their quantitative description with a detailed model including tip shape, elasticity of the sample, etc., is beyond the scope of this paper. Nevertheless, we like to stress that for the quantitative determination of the "true surface shape" $z_0(x,y)$ and indentation in conventional TM-AFM experiments such a detailed model is not needed.

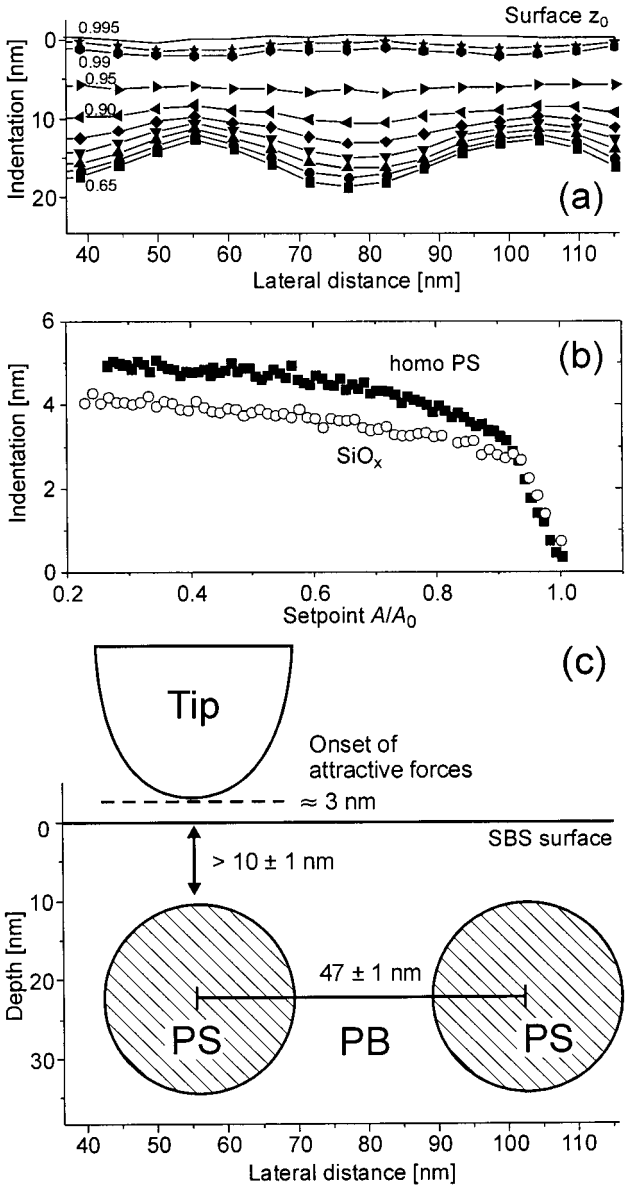

Figure 5. (a) Indentation for set points $A/A_0 = 0.995$, 0.990, 0.95, 0.90, 0.85, 0.80, 0.75, 0.70, and 0.65 as well as the "true surface" z_0 (data from one line of the 30 × 30 APD array; both axis have the same scale). (b) Indentation on silicon (free amplitude $A_0 = 55$ nm) and homopolystyrene (different tip, $A_0 = 45$ nm). (c) Proposed model for the near surface structure of the SBS sample (corresponding to the data shown in (a) and Figure 3; the cross section does not cut perpendicular through the PS cylinders).

Figure 5a shows the surface topography z_0 (topmost line) and the indentation depths Δz at *set points* A/A_0 ranging from 0.995 to 0.65. The figure shows data taken from a single line of the 30 × 30 APD curve array. One clearly sees that the indentation becomes more and more sinusoidal at lower *set points*, suggesting to draw spherical cylinder cross sections below the lines. This seems reasonable if one assumes that it is impossible for the tip to push the glassy PS cylinders deeper into the PB matrix.

Figure 5b shows two indentation curves taken on a silicon surface (using the same tip; $A_0 = 55$ nm) and on a thin film of homopolystyrene (using a different tip, $A_0 = 45$ nm). The surface of silicon is very hard; therefore, only small indentation is expected. Nevertheless, the indentation rapidly grows to 3 nm and then increases to about 4 nm at very low *set points*. Therefore, the *z*-position of the tip where attractive forces become measurable is roughly 3 nm apart from the point where the hard surfaces really touch each other, leading to the kink in the indentation. This distance may be due to a thin layer of water adsorbed on both the tip and the SiO_x surfaces and/or to a nonvanishing contribution of van der Waals forces. On homopolystyrene, a maximum indentation of 5 nm is found. This value is significantly smaller than the maximum indentation on the PS-rich phase of the SBS sample (some 15 nm).

In the following we like to compare this findings with the near-surface microdomain structure derived from crystallographic data (Figure 5c). The high indentation depths observed even on the harder parts of our sample indicate that the block copolymer surface is covered by a continuous layer of polybutadiene on top of the polystyrene cylinders. This is expected given that polybutadiene has a lower surface energy than polystyrene. The measurements of the indentation depth enable us to estimate the thickness of this PB surface layer. Considering that homopolystyrene could be indented by some 5 nm and that the hard region of the block copolymer sample could be indented by some 15 nm, one can estimate a PB layer thickness of $\geq 10 \pm 1$ nm. This certainly is a lower limit, since it is based on the assumption of infinite PB compressibility. This estimate for the PB layer thickness happens to agree quite well with the values expected for an ideal SBS surface of the given bulk structure. Given a diameter of 25 nm for the PS cylinders and an inter cylinder spacing of 45 nm, one calculates a thickness of 7 nm for the PB layer covering the topmost PS cylinders.

We are well aware of the limitations of such a quantitative evaluation of the TM-AFM data. One has to realize though that other techniques capable of determining the PB surface layer thickness with nanometer resolution (e.g., cross-sectional TEM or depth profiling) require complex sample preparation or do not have sufficient lateral resolution. Therefore, we feel that quantitative TM-AFM experiments can serve as an accurate while still simple technique for a quantitative characterization of the *native* near-surface morphology of soft materials.

Conclusion

We have investigated in detail the processes involved when soft polymeric materials are imaged with TM-AFM. In particular, we have presented a procedure to establish reliably with TM-AFM the true surface topography of a soft polymeric sample. The measurement of an array of APD curves enabled us to distinguish quantitatively between the "real" surface topography and lateral differences in tip indentation. We find that conventional TM-AFM height images are not necessarily reflecting the surface topography of the sample. In the case of the investigated SBS we find that the surface is flat and that conventional TM-AFM height images reflect lateral differences of tip indention. Changes in height and phase contrast could be attributed to the crossover between regimes where attractive and repulsive forces, respectively, dominate the tip−sample interaction. Laterally resolved quantitative determination of indentation depths finally enables one to estimate the thickness of "soft" surface layers on such tiny structures as block copolymer microdomains. In the case of SBS, the AFM results obtained in this way agree quantita-

tively with the microdomain spacing expected from crystallographic data.

We note that a sound determination of the real surface topography is of quite some importance for the comparison of experimental data with any model of a sample's subsurface structure—in particular, in numerical simulations aiming to predict near-surface morphologies of block copolymers and other complex fluids.[10,11] Flat boundaries are often used as they tend to simplify the simulations. Our results on SBS demonstrate that for this particular case the assumption of a planar interface between the block copolymer and the surrounding medium (air) is valid.

Finally, we have demonstrated that even on very soft polymeric samples TM-AFM can be applied as a quantitative and well-controlled analytical technique. What sometimes appears as artifacts in TM-AFM height and phase images can be related to the particular tip−sample interactions dominating in different *set point* regimes.

Acknowledgment. We gratefully acknowledge financial support through the Deutsche Forschungsgemeinschaft (SFB 481).

References and Notes

(1) Binnig, G.; Quate, C. F.; Gerber, C. *Phys. Rev. Lett.* **1986**, *56*, 930−933.
(2) Zhong, Q.; Inniss, D.; Kjoller, K.; Elings, V. B. *Surf. Sci.* **1993**, *290*, L688.
(3) Quist, A. P.; Ahlbom, J.; Reimann, C. T.; Sundqvist, B. U. R. *Nucl. Instrum. Methods B* **1994**, *88*, 164.
(4) Magonov, S. N.; Cleveland, J.; Elings, V.; Denley, D.; Whangbo, M.-H. *Surf. Sci.* **1997**, *389*, 201−211.
(5) Höper, R.; Gesang, T.; Possart, W.; Henneman, O.-D.; Bosek, S. *Ultramicroscopy* **1995**, *60*, 17−24.
(6) Pickering, J. P.; Vansco, G. J. *Polym. Bull.* **1998**, *40*, 549−554.
(7) Spatz, J. P.; Sheiko, S.; Möller, M.; Winkler, R. G.; Reineker, P.; Marti, O. *Langmuir* **1997**, *13*, 4699−4703.
(8) Kühle, A.; Sørensen, A. H.; Zandbergen, J. B.; Bohr, J. *Appl. Phys. A* **1998**, *66*, S329−S332.
(9) Turner, M. S.; Rubinstein, M.; Marques, C. M. *Macromolecules* **1994**, *27*, 4986−4992.
(10) Matsen, M. W. *J. Chem. Phys.* **1997**, *106*, 7781−7791.
(11) Huinink, H. P.; Brokken-Zijp, J. C. M.; Dijk, M. A. v.; Sevink, G. J. A. *J. Chem. Phys.* **2000**, *112*, 2452−2462.
(12) Stocker, W.; Beckmann, J.; Stadler, R.; Rabe, J. P. *Macromolecules* **1996**, *29*, 7502−7507.
(13) Konrad, M.; Knoll, A.; Krausch, G.; Magerle, R. *Macromolecules* **2000**, *33*, 5518−5523.
(14) Koneripalli, N.; Levicky, R.; Bates, F. S.; Ankner, J.; Kaiser, H.; Satija, S. K. *Langmuir* **1996**, *12*, 6681−6690.
(15) Morkved, T. L.; Jaeger, H. M. *Europhys. Lett.* **1997**, *40*, 643−648.
(16) García, R.; Tamayo, J.; Calleja, M.; García, F. *Appl. Phys. A* **1998**, *66*, S309−S312.
(17) Winkler, R. G.; Spatz, J. P.; Sheiko, S.; Möller, M.; Reineker, P.; Marti, O. *Phys. Rev. B* **1996**, *54*, 8908−8912.
(18) Tamayo, J.; García, R. *Appl. Phys. Lett.* **1997**, *71*, 2394−2396.
(19) Boisgard, R.; Michel, D.; Aimé, J. P. *Surf. Sci.* **1998**, *401*, 199−205.
(20) Nony, L.; Boisgard, R.; Aimé, J. P. *J. Chem. Phys.* **1999**, *111*, 1615−1627.
(21) Whangbo, M.-H.; Bar, G.; Brandsch, R. *Surf. Sci.* **1998**, *411*, L794−L801.
(22) Wang, L. *Surf. Sci.* **1999**, *429*, 178−185.
(23) Cleveland, J. P.; Anczykowski, B.; Schmid, A. E.; Elings, V. B. *Appl. Phys. Lett.* **1998**, *72*, 2613−2615.
(24) Chen, X.; Davies, M. C.; Roberts, C. J.; Tendler, S. J. B.; Williams, P. M.; Davies, J.; Dawkes, A. C.; Edwards, J. C. *Ultramicroscopy* **1998**, *75*, 171−181.
(25) Behrend, O. P.; Odoni, L.; Loubet, J. L.; Burnham, N. A. *Appl. Phys. Lett.* **1999**, *75*, 2552−2553.
(26) Bar, G.; Ganter, M.; Brandsch, R.; Delineau, L.; Wangbo, M.-H. *Langmuir* **2000**, *16*, 5702−5711.
(27) Kim, G.; Libera, M. *Macromolecules* **1998**, *31*, 2569.
(28) Kim, G.; Libera, M. *Macromolecules* **1998**, *31*, 2670.
(29) Wang, L. *Appl. Phys. Lett.* **1998**, *73*, 3781−3783.
(30) Luna, M.; Colchero, J.; Baró, A. M. *Appl. Phys. Lett.* **1998**, *72*, 3461−3463.
(31) Dorofeyev, I.; Fuchs, H.; Gotsmann, B.; Wenning, G. *Phys. Rev. B* **1999**, *60*, 9069−9081.
(32) Different procedures can be used to determine z_0. We find that the most reliable way is to determine first for large distances the mean phase $\langle\varphi\rangle$ and the corresponding standard deviation σ and then to take as z_0 the largest distance z of a phase vs distance curve at which $\varphi(z)$ deviates more than 2 σ from $\langle\varphi\rangle$. This introduces a systematic offset in the order of 0.3 nm and a mean error for z_0 of about one z-step (0.12 nm) of the measured $\varphi(z)$ curve.
(33) Delineau, L.; Brandsch, R.; Bar, G.; Whangbo, M.-H. *Surf. Sci.* **2000**, *448*, L179−L187.

MA001311X